Attenuation Constants of UHF Radio Waves in Arched Tunnels

YOSHIO YAMAGUCHI, MEMBER, IEEE, TAKEO ABE, MEMBER, IEEE, TOSHIO SEKIGUCHI, MEMBER, IEEE, AND JIRO CHIBA, MEMBER, IEEE

Abstract—**This paper describes the attenuation constants of UHF radio waves in arched tunnels. In the analysis, a point-matching method is combined with Muller's method and is applied to determine the propagation constant of the dominant mode. We compare the calculated result with previous experimental data, as well as that of the experimental equation and the theoretical result of a circular waveguide having the same cross-sectional area. Finally, an approximate equation for the attenuation constant is derived from the point-matching solution so that one can determine or estimate the value without elaborate calculations.**

I. Introduction

In recent years, many studies have been made of the propagation characteristics of radio waves in tunnels in the UHF band. From the theoretical point of view, tunnels can be regarded as hollow waveguides surrounded by a lossy dielectric medium, such as concrete, ground, and so on. In these studies, tunnels are modeled as hollow waveguides with circular [1]–[3], rectangular [4]–[5], and elliptical [6] cross sections.

The cross section of tunnels, in fact, is usually rectangular or arched-shaped. In the case of arched tunnels, a theoretical treatment of the propagation characteristics becomes somewhat difficult because the boundary does not coincide with a coordinate surface of an orthogonal coordinate system. For this reason, the arched tunnel is modeled in [7] and [8] as a circular waveguide having the same cross-sectional area. In addition, an experimental equation for the attenuation constant is derived from experimental results. Also, in [1] and [2], a theoretical calculation of the propagation constant has been presented according to this idea. However, there still remains the problem of whether the idea is correct or not, and, hence, there is a need to verify this result by another method. Three of the authors presented the propagation characteristics in arched tunnels [9] by a point-matching method combined with Newton's method, in which poor convergence of the propagation constant against the number of matching points was obtained. The number of matching points on a half boundary curve was chosen to be six to agree with the laboratory experimental result for the attenuation constant, without theoretical verification.

This paper extends the earlier work [9] and presents a new approximate equation for the attenuation constant in arched tunnels. The purposes of this study are:

1) to show the validity of the previous number of matching points in the convergence characteristics by Muller's method [11];
2) to show how the point-matching solutions agree with the experimental results [1], [7], [8], and to compare them with the theoretical results of an equi-area circular waveguide;
3) to present a simple and approximate equation for the attenuation constant based on the point-matching method so that one can determine or estimate the value with reasonable accuracy and without elaborate calculations.

Manuscript received December 3, 1984; revised March 18, 1985. This work was supported in part by the Sakkoukai Fund.

Y. Yamaguchi and T. Abe are with the Faculty of Engineering, Niigata University, Niigata 950-21, Japan.

T. Sekiguchi is with the Tokyo National Technical College, Tokyo 193, Japan.

J. Chiba is with the Faculty of Engineering, Tohoku University, Aoba Aramaki, Sendai, 980 Japan.

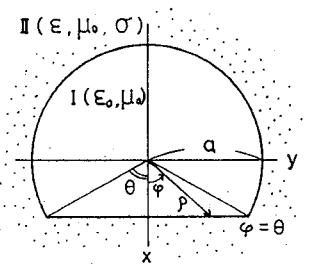

Fig. 1. Cross section of the arched tunnel and coordinate systems.

II. Point-Matching Solution

Fig. 1 shows the cross section of the arched tunnel to be considered here. The boundary curve is divided into two parts: circular ($\theta < |\varphi| < \pi$) and straight ($|\varphi| < \theta$) lines. The internal region of the boundary is composed of free space with permittivity ϵ_0 and permeability μ_0, and the external region is composed of a lossy dielectric medium with permittivity ϵ ($\epsilon_r = \epsilon/\epsilon_0$ relative dielectric constant), permeability μ_0, and conductivity σ.

Here, we present a brief summary of the point-matching method described in [9]. For the E_{11}^h mode, which corresponds to the dominant mode with horizontal polarization (transverse electric field is parallel to the y-axis in Fig. 1), the z-components of the electric and magnetic fields are written as

$$E_z = \sum_{n=0}^{\infty} A_n J_n(u\rho/a)\sin(n\varphi)\exp[j(\omega t - hz)]$$

$$H_z = \sum_{n=0}^{\infty} B_n J_n(n\rho/a)\cos(n\varphi)\exp[j(\omega t - hz)] \quad (1)$$

inside the boundary, and as

$$E_z = \sum_{n=0}^{\infty} C_n H_n^{(2)}(v\rho/a)\sin(n\varphi)\exp[j(\omega t - hz)]$$

$$H_z = \sum_{n=0}^{\infty} D_n H_n^{(2)}(v\rho/a)\cos(n\varphi)\exp[j(\omega t - hz)] \quad (2)$$

outside the boundary, where

$$u^2 = (k_1^2 - h^2)a^2 \qquad v^2 = (k_2^2 - h^2)a^2 \quad (3)$$

$$k_1^2 = \omega^2\epsilon_0\mu_0 \qquad k_2^2 = \omega^2\epsilon\mu_0 - j\omega\mu_0\sigma = k_1^2\epsilon_r^* \quad (4)$$

$$\epsilon_r^* = \epsilon_r - j\sigma/\omega\epsilon_0 \quad (5)$$

$h = \beta - j\alpha$ is the propagation constant, α is the attenuation constant, and β is the phase constant. Also, A_n, B_n, C_n, and D_n are unknown coefficients, $J_n(x')$ is the nth order Bessel function of argument x', and $H_n^{(2)}(y')$ is the nth order Hankel function of the second kind of argument y'. The above expansion may not be a complete representation of the fields, e.g., the fields may have to be represented by Bessel functions in the largest circle in the air, Hankel functions outside the smallest circle circumscribing the tunnel, and both Bessel and Neumann functions in the in-between medium. However, since the boundary is convex, and the results to be presented in the next section are reasonable, the above representation is used here.

0018-9480/85/0800-0714$01.00 ©1985 IEEE

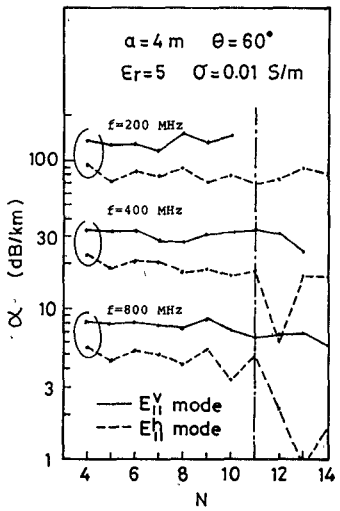

Fig. 2. Convergence characteristics of attenuation constant versus number of matching points by Newton's method.

The matching points are selected symmetrically about the x-axis, since the cross section is symmetrical about this axis. The points used to compute the results to be presented in Fig. 2 are

$$\varphi_n = \frac{(n-1/2)}{N}\pi, \qquad n = 1,2,\cdots,N \tag{6}$$

where N is the number of matching points. By matching the tangential field components along the boundary at the equi-angular points, $4N-2$ simultaneous homogeneous linear equations are obtained in a matrix form as

$$[Q][T] = 0 \tag{7}$$

where $[T]$ is column matrix of coefficients A_n, B_n, C_n, and D_n. The propagation constants then can be found by searching for the zeros of $\det[Q]$. In a similar manner, the $\det[Q]$ for the E_{11}^v mode corresponding to vertical polarization (transverse electric field is parallel to the x-axis in Fig. 1) can be obtained by interchanging $\sin(n\varphi)$ and $\cos(n\varphi)$ in (1) and (2) with each other.

Calculations were carried out based on Newton's and/or the Secant method, in which the complex variable u was adopted for the root of $\det[Q]=0$ instead of the normalized propagation constant [10]. As a numerical example, the attenuation constant against matching points N is shown in Fig. 2. Though poor convergence is seen in Fig. 2, six matching points have been adopted for the succeeding calculations, because the value of the attenuation constant at $N=6$ agrees well with the result of a laboratory experiment and is close to the average value at $N=5$ to $N=11$.

We reexamined the convergence properties by other methods in order to improve them. One method is to select the matching points at intervals equidistant along the boundary. Another is to use Muller's method [11] instead of Newton's to search for the zeros of the $\det[Q]$.

Fig. 3 shows how the convergence property can be improved in comparison with the one in Fig. 2. Muller's method is superior to Newton's method for this type of problem. An equidistant method seems to be better than an equiangular one. Attenuation constants by both sampling methods converge to a constant value at $N \geqq 11$, and the value at $N=6$ is almost the same as the asymptotic value at $N \geqq 11$. Hence, it is confirmed that the number 6 of the matching point has been appropriate for calculations.

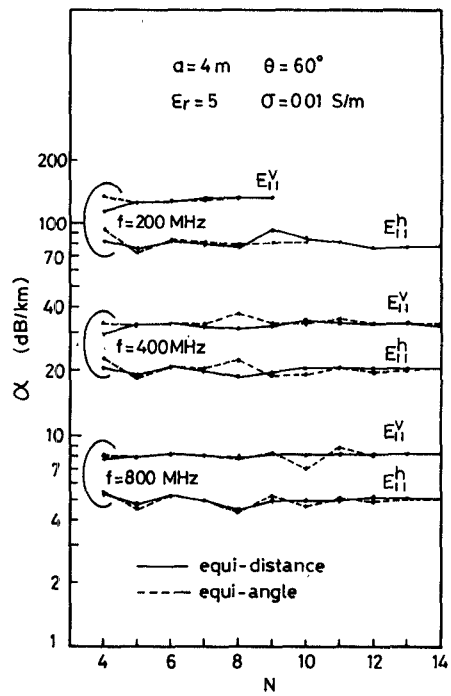

Fig. 3. Convergence characteristics of attenuation constant versus number of matching points by Muller's method.

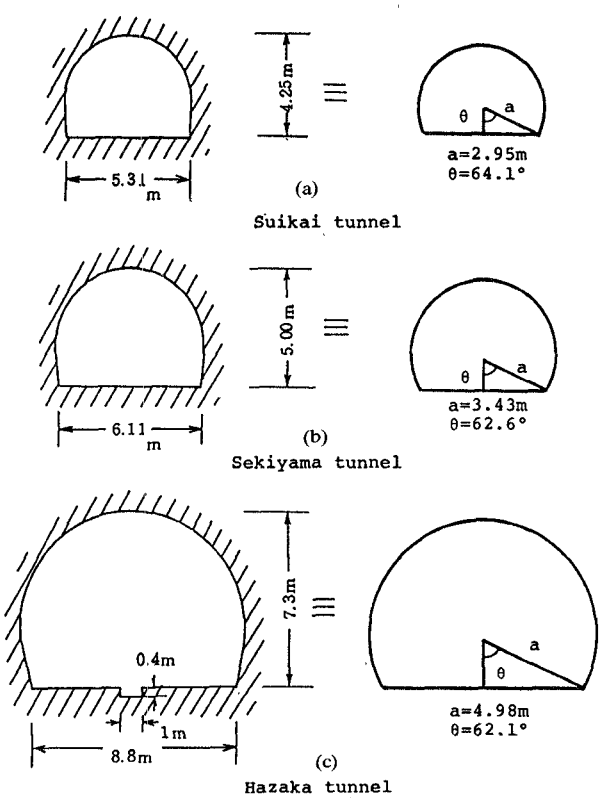

Fig. 4. The tunnel dimensions under measurement and equivalent dimensions of arched tunnels considered here.

III. Comparison with Experimental Results

We calculated the frequency characteristics of the attenuation constants in several arched tunnels in order to compare the results of the point-matching solution with previous experimental results [1], [7], [8]. The tunnel dimensions under experiment are

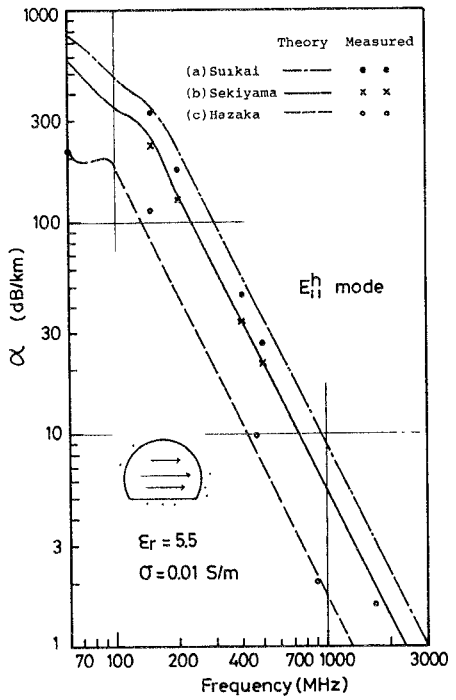

Fig. 5. Frequency characteristics of attenuation constant.

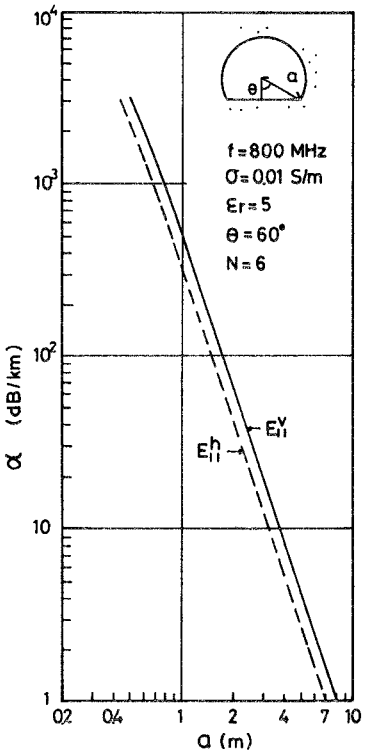

Fig. 6. Attenuation constant as a function of radius a.

shown in Fig. 4. The equivalent dimension parameters, radius a, and angle θ of the arched tunnel considered here are derived from the width and height of these tunnels in Fig. 4 so that they may have the same cross-sectional area, i.e.,

$a = 2.95$ m, $\theta = 64.1°$ for (a) Suikai tunnel,

$a = 3.43$ m, $\theta = 62.6°$ for (b) Sekiyama tunnel,

$a = 4.98$ m, $\theta = 62.1°$ for (c) Hazaka tunnel.

It is noted that the shape difference between the actual cross section and the present arched shape is very small.

Fig. 5 shows both the theoretical and experimental results. The calculated results are inversely proportional to frequency squared in the UHF band and agree well with experimental data.

IV. Comparison with the Results of Equiarea Circular Tunnels

An approximate equation for the attenuation constant in arched tunnels has been presented by Chiba [7] from the result of experiments. In formulating the equation, the arched tunnel is modified as a circular waveguide whose radius is chosen so that the cross-sectional areas are equal to each other. The equation is given in a simple form in the frequency range of 150–800 MHz, i.e.,

$$\alpha = 1460\frac{\lambda^2}{r^3} \quad \text{(dB/km)} \tag{8}$$

where λ is the free-space wavelength and r is the equivalent radius of the circular area (2.65 m $< r <$ 4.2 m).

According to (8), the attenuation constant is proportional to λ^2 and inversely proportional to r^3. Thus, we examine the validity of the experimental equation by the point-matching solution. As seen from Fig. 5, under the condition that r is somewhat larger than λ, the wavelength dependence applies. We calculated the attenuation constant as a function of radius a in order to verify the dimensional dependence. Fig. 6 shows the result for a frequency of 800 MHz, and shows that the attenuation constant

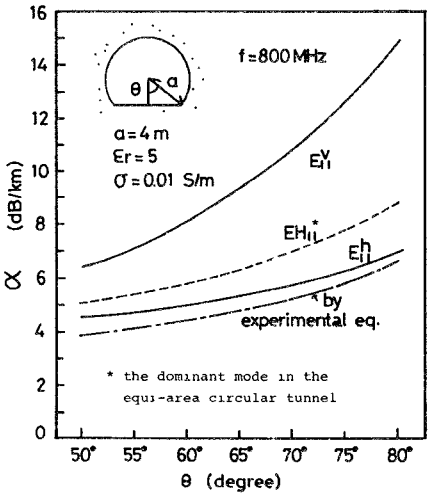

Fig. 7. Attenuation constant as a function of angle θ and comparison with the value in the equiarea circular tunnel

is inversely proportional to a^3. From Figs. 5 and 6, the experimental equation is confirmed to be appropriate as far as λ and r are concerned.

Equation (8), however, lacks information about polarization. This situation is the same for the circular tunnels. There are two dominant modes in arched tunnels corresponding to horizontal and vertical polarizations as mentioned in the previous section. It is necessary here to verify whether or not the attenuation constant in an equiarea circular tunnel is the same as in an arched tunnel. In this sense, the attenuation constants of the E_{11}^h and the E_{11}^v modes, shown in Fig. 7 as a function of angle θ, are compared with the attenuation constant given by (8) and the exact one of the corresponding dominant EH_{11} mode in the equiarea circular tunnel [3]. It is seen from Fig. 7 that the

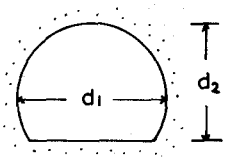

Fig. 8. Tunnel dimensions: width d_1, height d_2.

attenuation constant given by (8) almost agrees with that of the E_{11}^h mode. Hence, (8) is valid approximately for horizontal polarization characteristics in arched tunnels.

On the other hand, the exact attenuation constant of the EH_{11} mode in an equiarea circular tunnel is larger than that of the E_{11}^h mode and is smaller than that of the E_{11}^v mode. Though the value for the EH_{11} mode is closer to that of the E_{11}^h mode than E_{11}^v mode, the differences among the theoretical values of these modes become larger as the angle θ increases. This means, in the strict sense, that the idea of equiarea leads to errors. Disagreement between these values seems to be caused by the effect of tunnel dimensions relative to the wavelength according to polarization and material constants of the external medium. We will derive a new approximate equation in the next section based on the point-matching solution, taking account of these effects.

V. New Approximate Equation

The attenuation constant, in general, is a function of tunnel dimensions, frequency (or wavelength), polarizations, dielectric constant, and conductivity of the external medium. For UHF waves in a tunnel environment, the tunnel dimension is somewhat larger than the free-space wavelength. And the imaginary part of the relative dielectric constant in (5) may be neglected. This condition is applied to determine the propagation characteristics in rectangular tunnels [4], where the approximate equation for the attenuation constant is given. We rewrite the equation as follows.

For the dominant E_{11}^h mode with horizontal polarization

$$\alpha_h = 4.343\lambda^2\left(\frac{\epsilon_{r1}}{d_1^3\sqrt{\epsilon_{r1}-1}} + \frac{1}{d_2^3\sqrt{\epsilon_{r2}-1}}\right) \quad \text{(dB/m)} \quad (9)$$

and for the dominant E_{11}^v mode with vertical polarization

$$\alpha_v = 4.343\lambda^2\left(\frac{1}{d_2^3\sqrt{\epsilon_{r1}-1}} + \frac{\epsilon_{r2}}{d_2^3\sqrt{\epsilon_{r2}-1}}\right) \quad \text{(dB/m)} \quad (10)$$

where ϵ_{r1} is the relative dielectric constant of side walls, ϵ_{r2} is the relative dielectric constant of floor and roof, and d_1 and d_2 are the width and height of tunnels, respectively.

A similar result has been presented in circular dielectric waveguides analyzed for the optical spectrum region [12], i.e.,

$$\alpha = 5.09\lambda^2\left(\frac{\epsilon_r}{d^3\sqrt{\epsilon_r-1}} + \frac{1}{d^3\sqrt{\epsilon_r-1}}\right) \quad \text{(dB/m)} \quad (11)$$

where $d = 2a$ is the diameter of the circular waveguide.

One can see that the above equations (9)–(11) are in the same form except for the numerical coefficients, even though the cross sections are different. Therefore, we assume the same form of attenuation constant in arched tunnels with K_h, K_v instead of corresponding numerical coefficients in (9)–(11).

For the E_{11}^h mode

$$\alpha_h = K_h\lambda^2\left(\frac{\epsilon_r}{d_1^3\sqrt{\epsilon_r-1}} + \frac{1}{d_2^3\sqrt{\epsilon_r-1}}\right) \quad \text{(dB/m)} \quad (12)$$

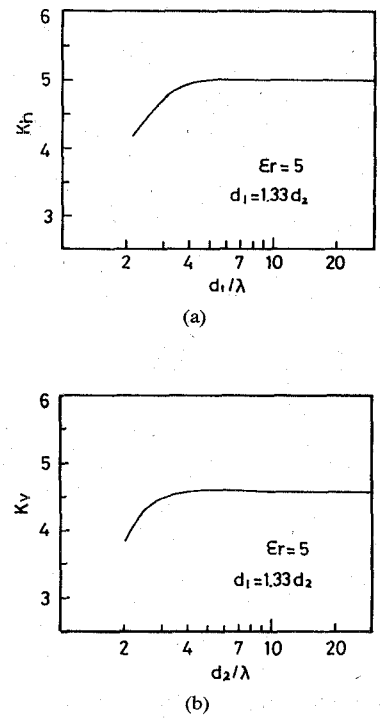

Fig. 9. Numerical coefficient versus tunnel dimension. (a) K_h, (b) K_v.

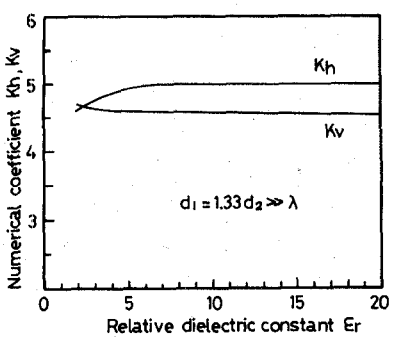

Fig. 10. Numerical coefficient versus relative dielectric constant.

and for the E_{11}^v mode

$$\alpha_v = K_v\lambda^2\left(\frac{1}{d_1^3\sqrt{\epsilon_r-1}} + \frac{\epsilon_r}{d_2^3\sqrt{\epsilon_r-1}}\right) \quad \text{(dB/m)} \quad (13)$$

where d_1 and d_2 are the maximum width and height, respectively, as shown in Fig. 8.

If the above equations holds true in the UHF band, the numerical coefficients K_h and K_v must be constant and independent of d_1, d_2, λ, and ϵ_r. In this sense, we calculated K_h and K_v by the point-matching method as functions of d_1/λ, d_2/λ, and ϵ_r. These values are shown in Figs. 9 and 10. It is seen in these figures that K_h and K_v approach constant values as d_1/λ or d_2/λ increases, and that K_h and K_v are indepdnent of ϵ_r ($\epsilon_r > 5$). This means that the equation holds under the condition that the width and height of a tunnel are larger than about four times the free-space wavelength.

The numerical coefficients K_h and K_v, on the other hand, depend on the cross-sectional shape or aspect ratio d_1/d_2. For most arched tunnels, the aspect ratio d_1/d_2 is in the range 1.3–1.6, or the angle θ in the 60°–80° (range). The values of K_h

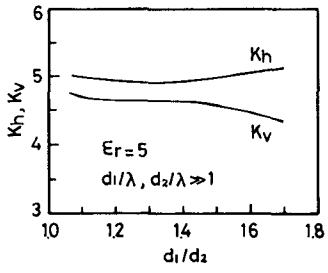

Fig. 11. Numerical coefficient versus aspect ratio of the arched tunnel.

and K_v are calculated in Fig. 11 as a function of aspect ratio d_1/d_2.

VI. Conclusion

We have presented the attenuation constants of the dominant modes corresponding to horizontal and vertical polarizations of the electric field in arched tunnels based on the point-matching method combined with Muller's method. The calculated values agree well with experimental results, and the validity of the previous experimental equation is confirmed theoretically for the horizontally polarized mode. Then, due to the fact that the difference in the attenuation constant between rectangular and circular tunnels is expressed only by a numerical coefficient in the approximate equations, we derived a similar equation for arched tunnels based on the point-matching solution considering polarization characteristics. The resultant equation can be used directly to determine or estimate the value for UHF radio frequencies.

Acknowledgment

The authors would like to thank Profs. N. Goto, Y. Naito, Y. Simizu, and T. Iijima, Faculty of Engineering, Tokyo Institute of Technology, for many helpful discussions and suggestions.

References

[1] J. Chiba, T. Inaba, Y. Kuwamoto, O. Banno, and R. Sato, "Radio communication in tunnels," *IEEE Trans. Microwave Theory Tech.*, vol. MTT-26, pp. 439–443, June 1978.

[2] T Inaba, Y. Kuwamoto, O. Banno, J. Chiba, and R. Sato, "Approximate solution of the attenuation constant of cylindrical tunnels," *Trans. IECE of Japan*, vol. J62-B, no. 4, pp. 435–436, Apr. 1979 (in Japanese).

[3] Y. Yamaguchi and T. Sekiguchi, "Propagation characteristics of normal modes in hollow circular cylinder surrounded by dissipative medium," *Trans. IECE of Japan*, vol. J62-B, no. 4, pp. 368–373, Apr. 1979 (in Japanese).

[4] A. G. Emslie, L. L. Robert, and P. F. Strong, "Theory of the propagation of UHF radio waves in coal mine tunnels," *IEEE Trans. Antennas Propagat.*, vol. AP-23, pp. 192–205, Mar. 1975.

[5] S. F. Mahmoud and J. R. Wait, "Geometrical optical approach for electromagnetic wave propagation in rectangular mine tunnels," *Radio Sci.*, vol. 9, no. 12, pp. 1147–1158, 1974.

[6] Y. Yamaguchi, T. Shimizu, and T Abe, "Propagation characteristics of the dominant mode in tunnels with elliptical cross section," *Trans. IECE of Japan*, vol. J64-B, no. 9, pp. 1032–1038, Sept. 1981 (in Japanese).

[7] J. Chiba, "Studies of helix," M.S. thesis, Faculty Eng., Tohoku Univ., Japan, pp. 32–185, 1957.

[8] J. Chiba, T. Inaba, Y. Kuwamoto, O. Banno, and R. Sato," Attenuation constants and phase constants of the tunnels," *Trans. 1987 ISAP Japan*, C-3-4, pp. 389–392, Aug. 1987.

[9] Y. Yamaguchi, T. Abe, and T. Sekiguchi, "Propagation characteristics of the dominant mode in tunnels," *Trans. IECE of Japan*, vol. J65-B, no. 4, pp. 471–476, Apr. 1982 (in Japanese).

[10] J. E. Goell, "A circular-harmonic computer analysis of rectangular dielectric waveguides," *Bell Syst. Tech. J.*, vol. 48, pp. 2133–2160, Sept. 1969.

[11] S D. Conte and C. de. Boor, *Elementary Numerical Analysis*, 3rd ed. New York: McGraw-Hill, 1981, ch. 3, pp. 120–125.

[12] E. A. J. Marcatili and R. A. Schmeltzer, "Hollow metallic and dielectric waveguides for long distance optical transmission and lasers," *Bell Syst. Tech. J.*, vol. 43, pp. 1783–1809, July 1964.

The Thermal and Spatial Resolution of a Broad-Band Correlation Radiometer with Application to Medical Microwave Thermography

JOSEPH C. HILL, MEMBER, IEEE, AND
RONALD B. GOLDNER, SENIOR MEMBER, IEEE

***Abstract*—The improved spatial and thermal resolution of a broad-band microwave correlation radiometer is discussed. Theoretical upper and lower bounds of the combined spatial and thermal resolution in a dense transmission medium are presented along with data obtained for two thermal sources in air. The application of broad-band correlation techniques to medical microwave thermography is novel, and the results indicate that electronic scanning of tissue should be possible.**

I. Introduction

Coherence theory [1] and its application to correlation radiometery [2], [3] has been discussed extensively in the literature and has been employed in radio astronomy for over 30 years. Because of its improved spatial resolution, correlation radiometry has received considerable interest in its application to medical microwave thermography [4]–[7].

Previous publications [4] have discussed a correlator employing a "pencil beam" antenna pattern formed by beam multiplication of partially overlapping antenna patterns, such as shown in Fig. 1(a), which permits examination of a small volume of tissue. However, examining an adjacent volume of tissue would require that the antennas be physically moved relative to the patient.

Recent publications [5], [6] have discussed measurements employing overlapping antenna beams as shown in Fig. 1(b). The enclosed volume of tissue, which is larger than that viewed by the "pencil beam" antenna pattern, should be able to be scanned electronically by introducing a delay in one arm of the correlator with the antennas stationary. Electronic scanning utilizing the radiometer delay [7] is distinct from aperture synthesis radiometery [8], in which the longitudinal coherence function, or mutual intensity function, is measured at several different locations by either antenna movement or antenna switching, with the radiometer delay set to zero [3]. Image reconstruction using aperture synthesis techniques is the microwave analogue of a van Cittert–Zernike experiment[1] in optics.

In this paper, we discuss the cross correlation of thermal radiation from two sources received by two antennas that are at a

Manuscript received October 15, 1984; revised March 18, 1985. This work was supported in part by a Tufts University biomedical research grant, HEW 1-SO7-RR07179-01 [7].

J. C. Hill is with Enon Microwave Inc, Topsfield, MA 01983.

R. B. Goldner is with the Department of Electrical Engineering, Tufts University, Medford, MA 02155.

[1]The van Cittert–Zernike theorem states that if the delay in the two paths of the correlator is much less than the reciprocal of the bandwidth, then the mutual intensity function, as measured across the detection plane, is equal to the Fourier transform of the brightness of the source distribution [1].

0018-9480/85/0800-0718$01.00 ©1985 IEEE